Article

Metal–azasterol complexes: Synthesis, characterization, interaction studies with DNA and TrxR and Biological Evaluation

Gonzalo Visbal,*[1,2] Angel Rubén Higuera-Padilla,[3] Luana Pereira Borba-Santos,[4] Wanderley de Souza,[5] Sonia Rozental[4] and Maribel Navarro*[1,6]

[1] Diretoria de Metrologia Aplicada *às* Ciências da Vida, Instituto Nacional de Metrologia, Qualidade e Tecnologia (INMETRO), Rio de Janeiro, Brazil.
[2] Centro de Desenvolvimento em Saúde (CDTS). Fundação Oswaldo Cruz – Fiocruz. Rio de Janeiro, RJ, Brazil.
[3] Laboratório de Química Bioinorgánica. Instituto Venezolano de Investigaciones Científicas (IVIC), Miranda, Venezuela.
[4] Laboratório de Biologia Celular de Fungos, Instituto de Biofísica Carlos Chagas Filho, Universidade Federal do Rio de Janeiro, Rio de Janeiro, RJ, Brazil.
[5] Laboratório de Ultraestrutura Celular Hertha Meyer, Instituto de Biofísica Carlos Chagas Filho, Universidade Federal do Rio de Janeiro, Rio de Janeiro, RJ, Brazil.
[6] Departamento de Química - Instituto de Ciências Exatas, Universidade Federal de Juiz de Fora (UFJF). Minas Gerais, MG, Brazil.
* Corresponding authors Email: gvisbal@gmail.com, maribel.navarro@ufjf.edu.br, maribelnava@gmail.com

Abstract. A new azasterol 22-hydrazine-imidazolin-2-yl-chol-5-ene-3β-ol (**AH3**) and their derivatives [Au(**AH3**)Cl] (**1**) and [Cu(**AH3**)$_2$(H$_2$O)$_2$](NO$_3$)$_2$ (**2**) were synthesized and characterized by a combination of elemental analyses, ^{1}H and ^{13}C -NMR, UV-vis and infrared spectroscopies. The interactions with two targets DNA and TrxR were investigated. The results from these studies suggested that these metal-azasterol complexes interact with DNA most probably by covalent binding. Complex **1** showed also the ability to strongly inhibit TrxR. Additionally, their activities against yeast cells of *Sporothrix spp.* were evaluated; finding that complex **1** was the most active, even better than itraconazole.
Keywords: Azasterol; gold; copper; DNA; thiorredoxin reductase; *Sporothrix spp*.

Resumen. Un nuevo azasterol 22-hidrazina-imidazolin-2-il-col-5-en-3β-ol (**AH3**) y sus derivados [Au(**AH3**)Cl] (**1**) y [Cu(**AH3**)$_2$(H$_2$O)$_2$] (NO$_3$)$_2$ (**2**) fueron sintetizados y caracterizados por técnicas espectros-copias como RMN ^{1}H ,^{13}C, UV-vis, infrarrojo y análisis elemental. Se investigaron las interacciones de estos compuestos sobre dos blancos moleculares el ADN y la TrxR. Los resultados encontrados sugirieron que estos complejos metal-azasterol interactúan con el ADN covalen-temente. El complejo **1** también mostró tener la capacidad de inhibir fuertemente la TrxR. Además, fueron evaluadas sus actividades contra *Sporothrix spp*., encontrando que complejo **1** fue el más activo, incluso mejor que el itraconazol.
Palabras clave: Azasterol; Oro; Cobre; Tiorreduxina reductasa; *Sporothrix spp*.

Introduction

Several research areas have looked for the identification of new drug targets. In the case of anti-fungi agents at least four major areas can be mentioned: i) Cell wall architecture, ii) Signaling pathways, iii) Cellular machinery, and iv) Plasma membrane composition [1].Within this context, one of our research efforts has been focused on the plasma membrane composition, be-cause several studies have demonstrated the potent effects of different ergosterol biosynthesis inhibitors (EBIs) on various pathogenic microorganisms, such as parasites and fungus, due to the fact that these agents interfere with some essential steps in the ergosterol biosynthesis pathway. Particular attention was given to inhibitors of Δ^{24}-sterol methyltransferase (24-SMT, an enzyme of ergosterol biosynthesis restricted to plants, protozoa, and fungi) that showed antimicrobial effects against *Trypanosoma cruzi*, *Leishmania donovani*, *Leishmania amazonensis*, *Leishmania mexicana, Pneumocystis carinii* (now *P. jirovecii*),

Paracoccidioides brasiliensis, *Candida spp*, and *Cryptococcus neoformans,* [2,3,4,5,6,7,8,9,10,11]. A new 24-SMT inhibitor belonging to the sterol hydrazone class, named 22-hydrazone-imidazolin-2-yl-chol-5-ene-3β-ol (H3) showed a significant anti-proliferative activity against the dimorphic fun-gus *Paracoccidioides brasiliensis* [9,12], and *Cryptococcus neoformans* [11]. More recently, its effects on the growth of *Sporothrix schenckii* and *Sporothrix brasiliensis* was described, and compared to that of itraconazole [13]. GC-MS analysis of cell sterol composition showed that sterols present in control cells (ergosterol and precursors) were replaced mainly by la-nosterol after H3 exposure. In contrast, itraconazole only par-tially inhibited ergosterol biosynthesis, and promoted accumulation of nine 14α-methyl sterols. Thus, inhibition of the enzyme 24-SMT showed a strong antiproliferative effect via disruption of ergosterol homeostasis, suggesting that this enzyme is a promising target for novel antifungal therapies against sporotrichosis.

Besides targeting the ergosterol in the membrane, our current interests are also focusing on the development of alternative chemotherapies against fungal and parasitic infection, based on the coordination of ergosterol biosynthesis inhibitors to metal-containing fragments, with the aim of enhancing their activity and diminishing their toxicity to human cells [14,15,16,17]. In fact, a variety of metal complexes based on this strategy have been already developed as anti-*Chagas diseases* [18,19] and leishmanicidal agents [18, 19, 20].

Recently, we reported the synthesis of platinum–sterol hydrazone complexes and their activities as anti-trypanosomatid [21]. The 24-SMT inhibitors used as ligands were 20-hydrazone-imidazoline-2-yl-5α-pregnan-3β-ol (H1) and 22-hydrazoneimidazoline-2-yl-chol-5-ene-3β-ol (H3 mentioned above). The results showed potent anti-trypanosomatid activity of the sterol hydrazone analogues and their platinum complexes. Likewise, H3 and trans-[Pt(H3)$_2$(Cl)$_2$] showed low cytotoxicity against human immunocompetent cells.

Encouraged by these findings, in current work we performed the synthesis and characterization of a new analogue of H3, the 22-hydrazine-imidazolin-2-yl-chol-5-en-3β-ol (sterol hydrazine class) (**AH3**, Fig. 1) and its two novel gold and copper derivatives (Fig. 2). Furthermore, we explored their possible interactions on two known important metallodrug targets such as DNA [22,23,24] and thioredoxin reductase (TrxR), particularly important for gold complexes [25,26,27,28,29]. In addition, their biological effects were evaluated on *Sporothrix* species, which is a fungal subcutaneous mycosis widespread in several countries, including Brazil [30]. The search for new and more effective antifungal drugs to treat sporotrichosis is becoming a priority, since no vaccine is currently available [31] and its current treatment is restricted to itraconazole [32], which has severe side effects, high costs and can result in the emergence of unresponsive clinical cases [33,34].

Results and Discussion

Synthesis and characterization

The azasterol **AH3** (See Fig. 1) was synthesized starting with 3β-hydroxy-23,24-bisnor-5-cholenic acid **I**, which was protected as a tetrahydropyranyl ether (THP) in THF as solvent and catalytic amounts of p-TsOH to obtain the intermediate **II** (Fig. 1). Without prior purification, reduction of the carboxylic acid group with lithium aluminium hydride (LiAlH$_4$) produced a primary alcohol **III** in 89% yield. Characterization of compound **III** has been determined previously [9]; nevertheless, it is important to note that the formation of methylene group in the side chain of the sterol will be important for the signal assignment of the side chain of the metal complexes. The new methylene group (H-22) appears as signals split into two multiple at 3.63 ppm and 3.34 ppm, indicating that they are not magnetically equivalent. Other two signals as multiples at 3.89 ppm and 3.51 ppm are due to H-5' equatorial of the THP group, and H-3 / H-5'axial of the THP group respectively. The ^{13}C-NMR

chemical shift of carbons C-3, C-22 and C-5'(THP) were 75.9, 68.0 and 62.7 ppm respectively. Conversion of the alcohol to the corresponding halide (bromide) was carried out using N,N,N′,N′-tetramethylethylendiamine, carbon tetrabromide and triphenylphosphine (Appel reaction) to obtain the intermediate **IV** with 96% yield. Deprotection of **IV** with HCl in refluxing ethanol, resulted in **V** in 98% yield. The ^{1}H-NMR shift data of the side chain allow unambiguous differentiation of the methylene protons (H-22). One of them had high field shifts from 3.63 ppm to 3.49 ppm, overlapping with H-3, while, the other proton remains in the same position at 3.32 ppm. In the ^{13}C-NMR spectrum of **V**, C-22 appears at 43.7 ppm indicating that bromine substitution effect shifts this carbon resonance to high-field.

Finally, the compound **V** was treated with 2-hydrazino-2-imidazoline hydrobromide and DBU in refluxing acetonitrile to afford the new 22-hydrazino-imidazolin-2-yl-chol-5-en-3β-ol (**AH3**) in 72% yield. The elemental analysis of the **AH3** was found in good agreement with the calculated data. The infrared spectra of **AH3** showed a sharp band at 1640 cm^{-1} corresponding to the stretching C = N of the hydrazino group. Likewise, the same spectrum showed broad band in the region 3000-3800 cm^{-1} associated to the stretching NH and OH at 3417 cm^{-1}. The ^{1}H-NMR spectrum of **AH3** in DMSO-d$_6$ showed on the low-field two signals singlet, one at 5.24 ppm due to H-6 olefin proton, another at 5.04 ppm due to one of the NH hydrazino group. H-22, H-24, H-25 and H-3 appeared as a broad complex signal in the range of 3.6 to 3.0 ppm. At high-field the spectrum showed a doublet at 1.01 ppm, and two singlets at 0.93 and 0.65 ppm assigned to the characteristic methyl groups, H-21, H-19 and H-18 respectively.

In the ^{13}C-NMR spectrum of **AH3,** C-23 (-C=N) of the imidazoline group appeared at 163.7 ppm, whereas, the carbons C-5 and C-6 of the sterol nucleus structure were observed at 141.28 and 120.3 ppm respectively. In addition, with the aid of COSY and HMQC data the side-chain of the **AH3** was unambiguously assigned, C-22 was observed at 57.5 ppm, indicating that nitrogen substitution effect shifts the carbon resonance to low-field. Likewise, C-24 and C-25 were assigned at 49.5 ppm. All structures described above were determined by comprehensive analyses of their elemental analyses, mass spectrometry, ^{1}H and ^{13}C NMR, COSY, HMQC, and IR spectroscopy data. The data are given in the experimental section.

In the same way, two new metal–**AH3** complexes [Au(**AH3**)Cl] (**1**) and [Cu(**AH3**)$_2$(H$_2$O)$_2$](NO$_3$)$_2$ (**2**) were synthesized by reaction of **AH3** with the appropriate metallic source under mild conditions, as summarized in the Fig. 2. Gold-azasterol complex (**1**) was synthesized at room temperature by the reaction between AuCl(THT) and the ligand **AH3** in dichloromethane for 96 hours. While, copper-**AH3** complex (**2**) was prepared by the reaction between Cu(NO$_3$)$_2$·3H$_2$O and **AH3** in methanol, under reflux for 2 hours. Both metal compounds were air-stable. Their elemental analyses were in agreement with the molecular formula proposed for these metal complexes (see experimental section).
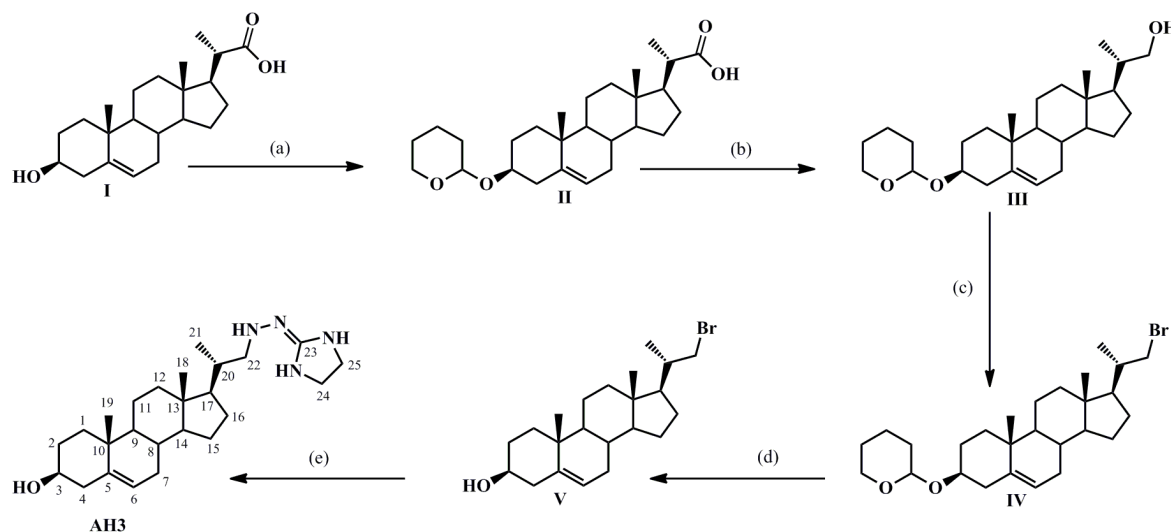
Fig. 1. Synthesis of **AH3**, a) THF, DHP, PTSA, rt (room temperature); b) THF, LiAlH4, 0 °C to rt; c) CH$_2$Cl$_2$, TMEDA, CBr$_4$, PPh$_3$, rt; d) EtOH, HCl, rt; e) CH$_3$CN, C$_3$H$_8$N$_4$ • HBr, DBU, reflux.

The IR spectra of these metal complexes showed frequencies distinctly associated with the main and characteristic functional group of the **AH3**, interestingly the band corresponding to stretching associated to NH and OH at 3417 cm^{-1} was clearly shifted to 3444cm^{-1} for both complex **1** and **2**. The band corresponding to the stretching C = N was shifted 6 cm^{-1} to lower frequency for both complex **1** and **2**. In addition, for complex **2** was also possible to observe a sharp band at 1384 cm^{-1} corresponding to the stretching vibrations of the nitrate (NO$_3$) group, which is characteristic for ionic nitrates complexes [35]. No bands in the region for coordinated nitrate were observed. The optical absorption spectra of the new metal complexes are essentially analogous to the free ligand, and they were characterized by intense absorption bands in the UV region characteristic of n→π* transitions of the imine group.

NMR signals could be assigned on the basis of 1D (^{1}H and ^{13}C NMR) and 2D (COSY and HMQC) data. It is worth pointing out, that NMR experiments were performed using DMSO-d$_6$. The ^{1}H and ^{13}C NMR chemical shift variation of each signal with respect to those of the free ligand (Δδ) were used as a parameter to deduce the mode of bonding of **AH3** to the metal. ^{1}H-NMR spectrum of complex **1** showed the presence of two singlets around of 0.65 and 0.93 ppm, corresponding to the H-18 and H-19 protons respectively. A signal doublet around 1.03 ppm belongs to the H-21. It was also observed a broad signal between 3.56 ppm and 3.0 ppm which was assigned to the methylene groups (H-22, H-24 and H-25) of the imidazoline and H3. Likewise, the olefin proton H6 and the singlet signal of NH group remain on their chemical shift at 5.24 ppm and 5.04 ppm respectively; in general all signals corresponding to **AH3** were displayed in the ^{1}H-NMR spectrum of the complex **1**, indicating that this ligand was coordinated to gold. However, the peak corresponding to protons H-22 (which are the protons expected to shift, due to the coordination to Au atom) is

overlapped with other protons (above mentioned) and the water protons of DMSO-d$_6$, making it difficult to calculate the chemical shift variation with respect to those of the free **AH3**. Interestingly, in the ^{1}H-NMR spectrum of complex **2** it was possible to assign some chemical shifts, although, it is a paramagnetic complex.

On the other hand, all signals in the ^{13}C-NMR spectrum for complex **1** were assigned, selected data ^{13}C-NMR are given in Table1. It was noticeable that the peaks of C-22, C-23, C-24 and C-25 were clearly shifted 8.0, 2.2 and 7.3 ppm upfield with respect to those of the free ligand, the rest of the signals showed no significant shifts. Similar behaviour was observed for complex **2** (see Table 1). These effects suggest that **AH3** is coordinated to both gold and copper through the nitrogen atom of the C=N exocyclic of the imidazol ring, a good donor site in this molecule (Fig. 2).

According to the available data, the formulation proposed for the new gold-azasterol compound **1** corresponds to 14-electron Au(I) complex in a lineal coordination geometry, while the structure of complex **2** corresponds to 17-electrons Cu(II) in a tetragonal coordination geometry (Fig. 2).[36]

DNA interaction studies

The ability of metal–**AH3** complexes to interact with DNA, an important bio-target, was examined using several physical chemical techniques that can supply information and give clear vision with respect to the interaction that is taking place between them [37,38, 39]. For this, we performed UV-visible absorption titration in order to determine the equilibrium binding constant (K$_b$) of the **AH3** and its metal derivatives **1** and **2** with ct-DNA, monitoring the perturbation of the absorption electronic spectrum of each compound after the addition of ct-DNA

Table 1. Selected ^{13}C-NMR Data for metal-azasterol complexes

Comp.	AH3 (ppm)	[Au(AH3)Cl] (1) (ppm)		[Cu(AH3)$_2$(H$_2$O)$_2$](NO$_3$)$_2$ (2) (ppm)	
Asig.	δ	δ	$\Delta\delta$	δ	$\Delta\delta$
C23	163,7	161.5	2.2	ND	-
C22	57.5	49.5	8.0	55.5	2.0
C24, C25	49.6	42.3	7.3	42.2	7,4
C21	19.0	19.0	0.0	ND	-

ND: no detected.
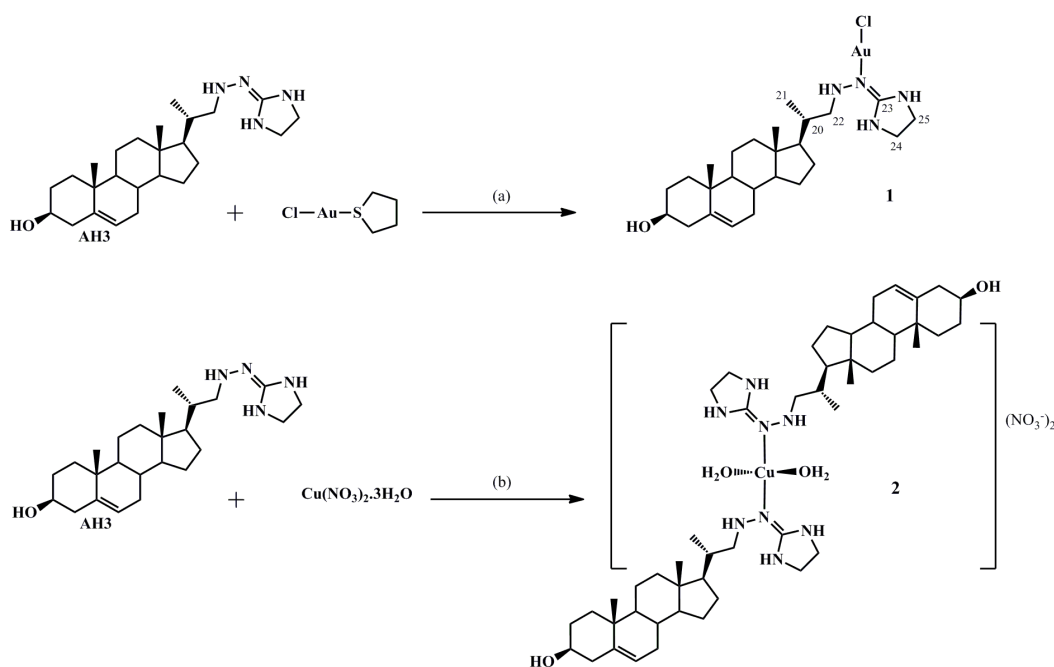
Fig. 2. Synthesis of the new azasterol-metal complexes **1** and **2**. (a) CH$_2$Cl$_2$, rt, 96h; (b) MeOH, Δ, 2h.

and using the equation described in the Experimental Section. The hypochromism, bathochromic shift and corresponding binding constants (K$_b$) for all compounds are presented in Table 2. It is worth mentioning that the absorption spectra of **AH3** and complex **2** with increasing concentrations of ct-DNA showed similar behaviour (Fig. 3). A significant decrease in their absorption intensity was observed for both compounds, showing hypochromism around 50 % and 39% respectively. The K$_b$ values obtained for **AH3** and complex **2** are within the interval for compounds which have moderate binding affinity with the DNA [40, 41], whilst complex **1** exhibited slight hypochromism (about 5%) upon addition of ct-DNA.

In order to collect further information on the interaction of these compounds with the DNA, we determined the melting temperature (T$_m$) from the thermal denaturation curves of DNA (Figure 4) obtained as described in the Experimental Section. The melting temperature for the DNA alone was 80.5 °C, while the T$_m$ for ct-DNA in the presence of **AH3** and complexes **1** and

2 were 80.0, 78.0 and 79.5 °C respectively. A slight decrease of T$_m$ was obtained for **AH3**, while significant decrease was observed for complexes **1** and **2** (Table 2) indicating that the interaction of these metal complexes with ct-DNA leads to a destabilization of the double helix of DNA [42].

Viscosity measurements are considered as one of the most unambiguous methods to determine intercalation or non-intercalation binding of complexes to DNA, due to the viscosity experiments reveal changes in the length of the DNA double helix [43]. The results of the viscosity measurements for **AH3** and complexes **1** and **2** are shown in Fig. 5. **AH3** showed slightly decreased in relative viscosity of the DNA, while complexes **1** and **2** decreased markedly the CT-DNA solution viscosity indicating that these compounds do not intercalate the bases of the DNA molecule [44]. Similar behaviour to that observed for complexes **1** and **2** have been reported for compounds that form bond with DNA helix, such as cisplatin [45].
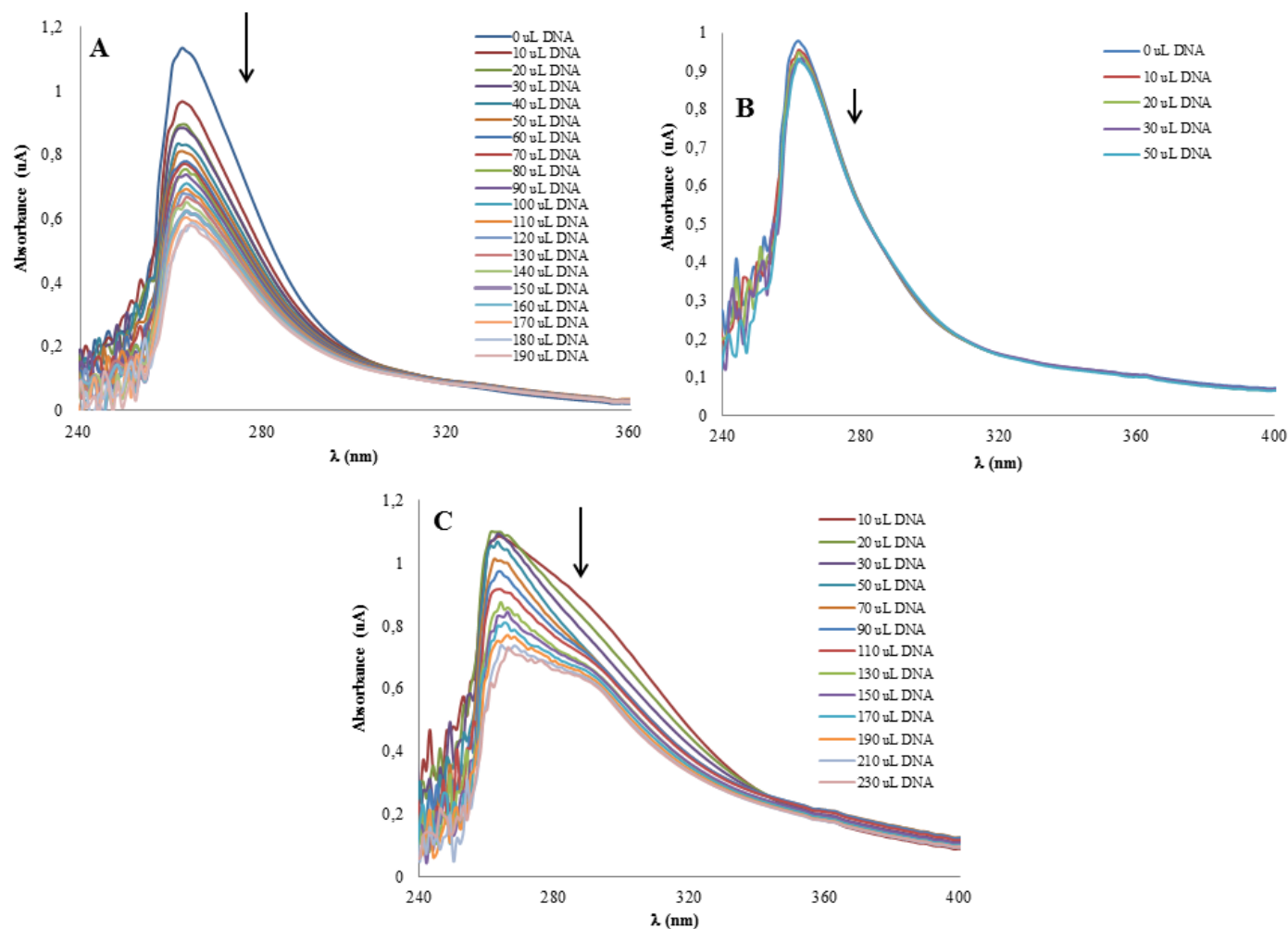
Fig. 3. Spectrometric titration spectra of **AH3**(A), complex **1** (B) and complex **2** (C). [compound] = **5x10^{-4}M** and [DNA] 0-150 μM.
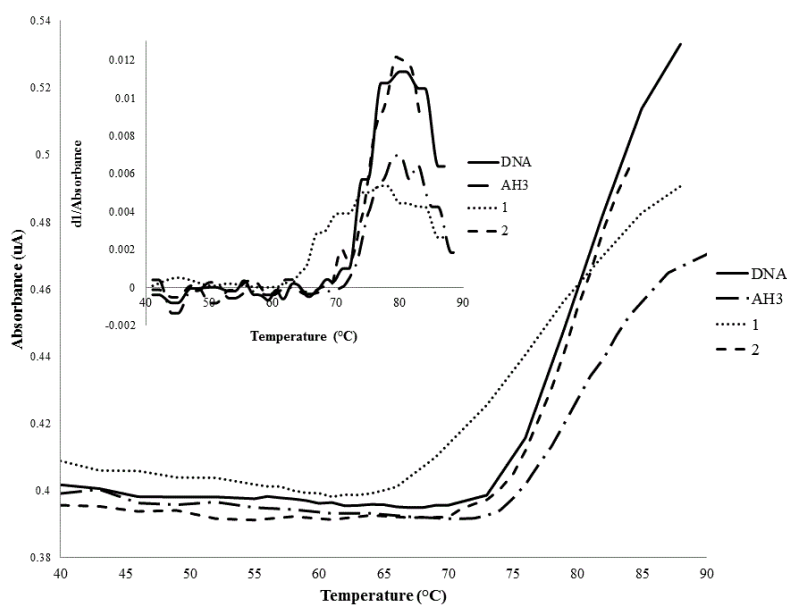
Fig. 4. Melting curves of DNA alone and in the present of the **AH3** and complexes **1** and **2** (Ri = 0.1 (relation [Compound]/[DNA]), incubated for 1h at 25°Cin 50 mM NaClO$_4$ and 5 mMTris/HCl buffer (pH = 7.29).

Table 2. Data obtained for the binding constants (K_b), hypochromism, Red shift and melting temperature (T_m) for interaction of **AH3** and complexes **1-2** with DNA.

complexes	K_b (mol L^{-1})$^{-1}$	(%) hypochromism	Red shift nm (λ)*	ΔT_m (ºC)
AH3	2.0×10^3	50	4 (264)	−0.5
1	0.3×10^3	5	0 (262)	−2.5
2	1.1×10^3	39	4(262)	−1.0

* The peak corresponding to the red shift is shown in brackets. T_m for DNA alone was 80.5 ºC.

Based on the changes of absorbance, thermal denaturation and viscosity obtained complexes **1** and **2**, together with the good similarity observed when comparing their data with those well known for cisplatin interacting with the DNA, we suggest that these metal complexes could bind covalently to DNA. It is possible to envisage a metal complexes-like mechanism involving solvation of the chloride in the case of complex **1** and nitrate for complex **2**, and most likely to result in a covalent bonding between the metal and a DNA base. Studies to confirm the covalent binding will be performed in the future.

Thioreducin reductase (TrxR) interaction studies

Thioredoxins are the major cellular protein disulfide reductases and are responsible for the regulation of numerous biochemical processes within the cell [46], since it is an essential enzyme for the efficient maintenance of the cellular redox homeostasis. Therefore, it should be considered as an attractive target for metallodrugs [26,47]. Various gold complexes showed strong affinity for TrxR allowing deactivation due to the formation of a covalent bond to the selenium center of the enzyme [27].

The inhibitory potential of **AH3** and their gold (**1**) and copper (**2**) complexes were studied using the dithiobisnitrobenzoic acid (DTNB) reduction assay using isolated rat liver TrxR. This assay makes use of the fact that TrxR reduces the disulfide bonds of DTNB with formation of 2-nitro-5-thionitrobenzoic acid (TNB), which can be detected photometrically. The IC$_{50}$ values for **AH3**, **1** and **2** were calculated using the data from the plots of the formation of TNB versus time for each compound (Fig. 6A and 6C), which are related to the percentage of the TrxR activity of each compound relative to the control (Fig. 6B and 6D). Complex **1** inhibited the enzyme activity at nanomolar concentrations (IC$_{50}$ = 22.2 nM), while **AH3** and **2** did not inhibit TrxR, even at the highest concentrations (>500 µM). Clearly, complex **1** was the best inhibitor of this kind of compound, indicating that inhibition of TrxR is selective for gold complexes as it has been reported by other researchers [26-29], since this could bind to the selenium atom in the active site of the enzyme, thereby inhibiting its ability to oxide-reduction [48].

Lipophilicity determination

The partition coefficient (log P) is defined as the ratio of the equilibrium concentrations of a substance dissolved in a biphasic system which consists of two largely immiscible (water or buffer and n-octanol). It is the most widely used method for measuring the chemical compound's lipophilicity [49]. This value is determinative of the potential pharmacological use of drugs, since it has a great influence on the absorption properties, distribution, metabolism, and excretion of the drug in the body. Additionally, it is well known that the hydrophobic effect is the greatest driving force for binding of drugs to their targets [50]. As shown in Table 3, the values of log P obtained for **AH3** and **1** were 0.11 and 0.35, indicating that these compounds have preference for the organic phase (octanol), revealing its lipophilic behaviour [51]. Because of this feature, such compounds may penetrate the cell membrane, which is mainly formed by lipids, and then perform their respective biological action. With respect to complex **2**, log P value was -0.39, implying that this compound has preference for the aqueous phase, with hydrophilic behaviour [52]. This fact can be attributed to the ionic characteristic of the complex **2**, and suggests that this copper complex as a potential drug could be delivered directly into the bloodstream [53].

Since there is an important need to design and develop drugs that intercept cellular pathways that involve identified drug targets for relevant diseases such as pathogenic infection, genetic disorders, among others, we decided to establish
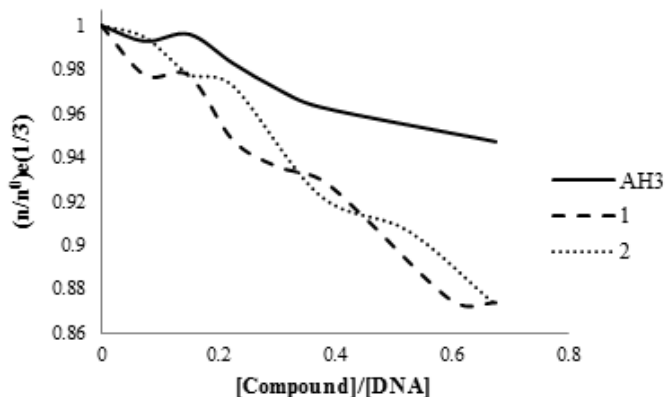
Fig. 5. Effect of increasing concentration of the complexes on the relative viscosity of DNA at 25 °C.
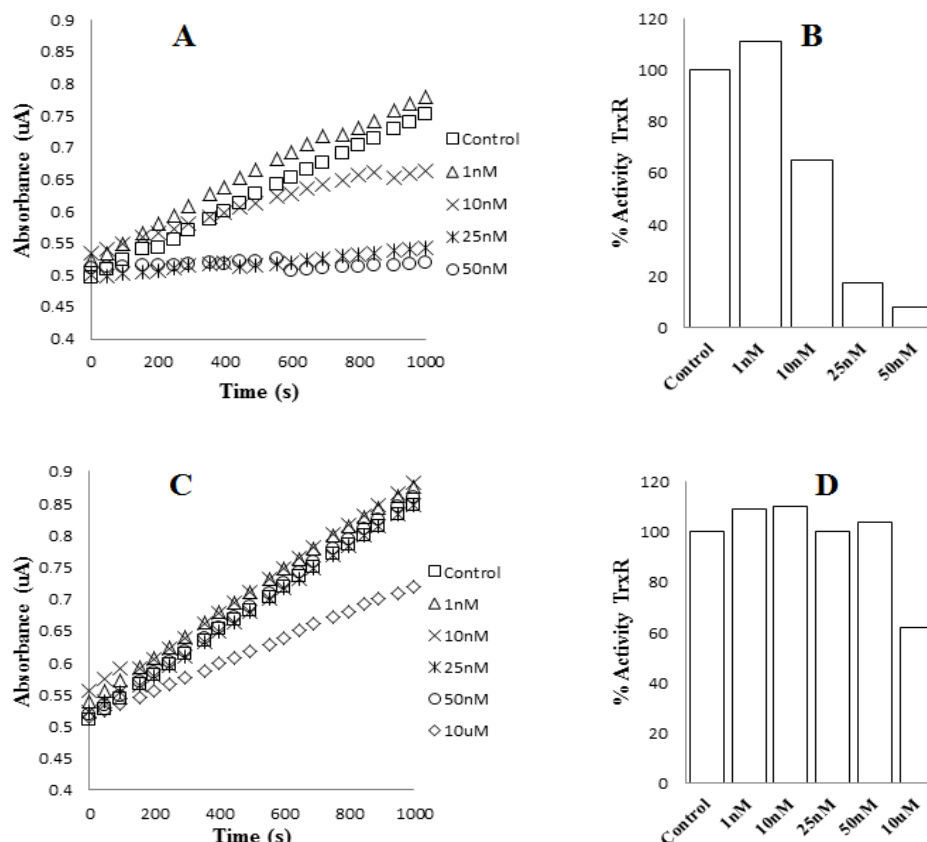
Fig. 6. Inhibition of the thioredoxin reductase activity by compounds **1** and **2.**

Table 3. Experimental Log *P* values of compounds **AH3, 1** and **2.**

Compound	Log *P*
AH3	0.11
1	0.35
2	-0.39

whether the new metal-**AH3** derivatives interact with DNA, an important biological target for different illnesses, as well as study the inhibition of another important target like TrxR, particularly for gold complex. Below we present the first screening of their pharmacological potential against the fungus *Sporothrix spp.*

Biological Activities

Antiproliferative activity to fungal cells

Antifungal activity of azasterol (**AH3**) and its metal complexes [Au(**AH3**)Cl] (**1**) and [Cu(**AH3**)$_2$(H$_2$O)$_2$](NO$_3$)$_2$ (**2**) were evaluated against yeasts of the reference isolates *S. schenckii* CBS 132984 and *S. brasiliensis* CBS 133021. Minimum inhibitory concentration (MIC) values – the lowest concentration of the

compound that inhibits fungal growth – were determined (Table 4).

All compounds were highly effective against the tested yeast, with MIC in the high nanomolar or low micromolar range. The biological activity of the **AH3** is found to be the same than that of the itraconazol standard antifungal. Indeed, both compounds showed a MIC = 2.5 μM against the CBS 132984 strain, and a MIC = 1.25 μM against the CBS 133021 strain.

Cu(II) complex (**2**) showed similar fungal activity against both yeast strains with a MIC of 2.5 μM. Moreover, comparing its activity with **AH3**, it is possible to see that the copper atom did not modify the activity of the azasterol. In contrast, Au(I) complex (**1**) showed marked activity, exhibiting MIC values of 0.3 and 0.16 μM against *S. schenckii* and *S. brasiliensis* respectively.

It is important to highlight that **AH3** was synthesized as analogue of azasterol H3 (Sterol hydrazone class), because it has shown a significant anti-proliferative activity against *S. schenckii* and *S. brasiliensis*, even better than itraconazole [13]. Thus, it can be seen from Table 4 that, this new azasterol called **AH3,** also inhibited fungal growth at low micromolar concentration. In addition, we can say that the antifungal potency displayed by AuCl(**AH3**) (**1**) is approximately 8-fold higher than **AH3** and itraconazole, thus indicating that our strategy for the

Table 4. Susceptibility of *Sporothrix schenckii* and *Sporothrix brasiliensis* yeasts to compounds **AH3**, **1** and **2**, compared to itraconazole.

Compounds	Minimum inhibitory concentration (μM)	
	S. schenckii	S. brasiliensis
AH3	2.5	1.25
[Au(**AH3**)Cl] (**1**)	0.3	0.16
[Cu(**AH3**)$_2$(H$_2$O)$_2$](NO$_3$)$_2$ (**2**)	2.5	2.5
Itraconazole	2.5	1.25

development of new alternative chemotherapies against fungal infection based on the coordination of ergosterol biosynthesis inhibitors to metal-containing fragments, with the aim of enhancing their activity, was correct.

In Brazil, sporotrichosis is a serious public health problem, principally in Southeast Brazil, mainly due to feline transmission [54]. *S. schenckii* and *S. brasiliensis* are the most pathogenic *Sporothrix* species, and more frequently isolates in Brazil [55]. In the cases of *S. brasiliensis*, treatment with itraconazole is often not effective [56]. Thus, [Au(**AH3**)Cl] (**1**) is a compound with potential for development of new antifungal agent for sporotrichosis treatments. However, additional studies are needed to evaluate *in vivo* efficacy and safety of this molecule.

Conclusion

Three new compounds were synthesized and characterized through elemental analysis, UV-Vis, IR and NMR as described here. The new azasterol (**AH3**) was coordinated to different metals such as Au and Cu. These metal-AH3 derivatives most probably interact with the DNA via covalent binding. Only complex **1** inhibits TrxR. **AH3** and complex **1** are lipophilic compounds, while complex **2** showed a hydrophilic behaviour. The activities of these metal complexes were investigated against fungus causing sporotrichosis. Our results showed that all compounds were highly effective against the tested yeast. Gold-AH3 complex was the most promising agent for the development of new anti-sporotrichosis compound.

Experimental Section

General Procedure

All manipulations were routinely carried out under N$_2$ using common Schlenck techniques. Solvents were purified using standard procedures immediately prior to use. Melting points were measured on a Buchi apparatus and are uncorrected. C, H and N analyses were performed with a Carlo Erba EA1108 elemental analyzer. The NMR spectra were obtained in CDCl$_3$ and in a DMSO-d$_6$ solution in a Bruker AVANCE 300 spectrometer. ^{1}H NMR shifts were recorded relative to residual proton resonances in the deuterated solvent. IR spectra were

obtained with a Nicolet Magna IR 560 spectrometer. UV–vis spectra were recorded on a HP 8453 diode array instrument.

Synthesis of the new sterol hydrazine and its derivatives of gold and copper

3β-tetrahydropyraniloxy-23,24-bisnor-5-cholenic acid (**II**)
3β-hydroxy-23,24-bisnor-5-cholenic acid **I** (1.807 g; 5.22 mmol) was suspended in tetrahydrofuran (THF, 10 mL). 3,4-[2H]-dihydropyran (2.36 mL; 26.04 mmol) and catalytic amount of p-toluenesulfonic acid hydrated (210 mg; 1.10 mmol) were added. The solution was stirred at room temperature for 24 hours, becoming a dark yellow solution. To this solution were added 20 mL of NaHCO$_3$ and 10 mL of CH$_2$Cl$_2$. The aqueous phase was extracted 3 times with portions of 20 mL of dichloromethane. The resulting organic phase was acidified with 5 mL of CH$_3$COOH and washed 3 times with 50 mL of water, then dried with Na$_2$SO$_4$ and concentrated. (2.156 g, 96%). ^{1}H NMR (CDCl$_3$, 500 MHz) δ 5.32 (1H, t, H-6), 4.71 (1H, t, H-1'), 3.90 (1H, m, H-5'), 3.48 (2H, m, H3 and H-5'), 1.22 (3H, d, *J* = 6.81 Hz, H-21), 0.99 (3H, s, H-19), 0.68 (3H, s, H-18).

3β-tetrahydropiraniloxy-23-bisnorchol-5-en-22-ol (**III**)
To a solution of 3β-tetrahydropyranyloxy-23,24-bisnor-5-cholenic acid (**II**) (1.0 g; 2.32 mmol) in dry tetrahydrofuran at 0 °C was added LiAlH$_4$ (91.1 mg; 2,40 mmol). This solution was placed under stirring and then allowed to heat at 25 °C for 12 hours. The reaction was stopped with water in an ice bath. The reaction was extracted with 3 portions of 15 mL of chloroform and then the organic phase was washed with 3 portions of water. Dried with Na$_2$SO$_4$, then filtered, concentrated and purified through silica gel column with a mixture of solvent hexane: ethyl acetate 4:1. (861 mg, 89%). ^{1}H NMR (CDCl$_3$, 500 MHz) δ 5.32 (1H, t, H-6), 4.69 (1H, t, H-1´), 3.89 (1H, m, H-5´), 3.63 (1H, m, H-22), 3.49 (2H, m, H-3 and H-5´), 3.34 (1H, m, H-22), 1.03 (3H, d, *J = 6.57* Hz, H-21), 0.99 (3H, s, H-19), 0.68 (3H, s, H-18).

3β-tetrahydropyranyloxy-23-bisnorchol-5-en-22-bromine (**IV**)
N,N,N',N'-tetramethyl ethylenediamine (270 μL; 1.80 mmol), carbono tetrabromide (655 mg;1.98 mmol) and triphenylphosphine (572 mg; 2.18 mmol) were added to a solution of 3β-tetrahydroxipyraniloxy-23-bisnorchol-5-en-22-ol (**III**) (680 mg; 1.63 mmol) in dry dichloromethane. The solution was left

under constant stirring at room temperature for one hour, noticing a yellow solution. This solution was concentrated, dissolved in ethyl acetate and passed through a silica gel column using as mobile phase hexane: ethyl acetate 6:1. (751 mg. 96%). ^{1}H NMR (CDCl$_3$, 500 MHz) δ 5.32 (1H, t, H-6), 4.68 (1H, t, H-1′), 3.89 (1H, m, H-5′), 3.49 (3H, m, H3, H-5′ and H-22), 3.34 (1H, m, H-22), 1.07 (3H, d, *J = 6.45* Hz, H-21), 0.98 (3H, s, H-19), 0.68 (3H, s, H-18).

22-bromine-23-bisnorchol-5-en-3β-ol (**V**)

To a solution of 3β-tetrahydropyranyloxy-23-bisnorchol-5-en-22-bromine **IV** (749 mg;1.56 mmol) in ethanol (25 mL) was added concentrated hydrochloric acid (1 mL; 10.15 mmol) and placed under reflux for 30 minutes. Acid was neutralized with 1N sodium hydroxide, and extracted with 3 portions of chloroform. Then organic phase was concentrated and a white solid was precipitated. (605 mg. 98%). ^{1}H NMR (CDCl$_3$, 500 MHz) δ 5.32 (1H, t, H-6), 3.48 (2H, m, H-3 and H-22), 3.32 (1H, m, H-22), 1.07 (3H, d, *J = 6.48* Hz, H-21), 0.98 (3H, s, H-19), 0.68 (3H, s, H-18).

22-hydrazine-imidazolin-2-yl-chol-5-en-3β-ol (**AH3**)

A solution of 2-hydrazine-2-imidazoline hydrobromide (197 mg; 1.09 mmol) and 1,8-diazabicyclo [5.4.0] undec-7-ene (DBU) (161 µL; 1.08 mmol) in acetonitrile (15 mL) was placed under stirring for five minutes, then 22-bromine-23-bisnorchol-5-en-3β-ol (**V**) (150 mg; 0.38 mmol) was added, and placed under reflux for 24 hours. After this time the solution was concentrated, dissolved in butanol and washed with saturated sodium chloride. The organic phase was concentrated and washed with a solution of hexane: ethyl acetate 4:1, then diethyl ether, and finally dried under vacuum. A light orange solid was obtained. (113 mg, 72%). Amorphous power: mp 230-232 °C; IR (KBr) ν$_{max}$ 3417, 2933, 2866, 1640 cm^{-1}. ^{1}H NMR (DMSO-d$_6$, 500 MHz) δ 5.25 (1H, t, H-6), 5.04 (1H, s, NH), 3,56 (4H, s, H-24 and H-25), 1.01 (3H, d, *J = 6.70* Hz, H-21), 0.93 (3H, s, H-19), 0.65 (3H, s, H-18). ^{13}C RMN (DMSO-d$_6$) δ 163.73 (C-23), 141.25 (C-5), 120.36 (C-6), 69.98 (C-3), 56.04 (C-22), 42.36 – 42.21 (C2-4, C-25), 19.01 (C-21), 16.98 (C-19), 12.11 (C-18). ε$_{(264nm, DMSO)}$ = 2840 M^{-1}cm^{-1}. ESI-MS (MeOH) m/z: 415 M$^+$. *Anal*. C 63.34%, N 11.94%, H 10.35%, calcd for C$_{25}$H$_{42}$N$_4$O·3.5H$_2$O, C 62.86%, N 11.73%, H 10.34%.

Chloro(22-hydrazine-imidazolin-2-yl-chol-5-en-3β-ol)gold(I) (**1**)

To a solution of (chloro(tetrahydrothiophene)gold (108.0 mg; 0,34 mmol) in dry dichloromethane was added **AH3** (145,0 mg; 0,38 mmol). The solution was left under constant stirring at room temperature for 96 hours. A violet solid after filtration was obtained. Then it was washed with three solvents as follow, first dichloromethane, second acetonitrile, third diethyl ether, and finally dried under vacuum. (175 mg, 49%). Amorphous power: mp 278-280 ºC; IR (KBr) n$_{max}$ 3441, 2934,1634 cm^{-1}. ^{1}H-NMR (DMSO-d$_6$, 500 MHz) δ 5.25 (1H, t, H-6), 5.09 (1H, s, NH), 3.33 (4H, s, H-23 and H-24), 0.82 (3H, d, *J = 6.95* Hz,

H-21), 0.93 (3H, s, H-19), 0.69 (3H, s, H-18). ^{13}C-NMR (DMSO-d$_6$) d161.48 (C-23), 141.27 (C-5), 120.32 (C-6), 69.98 (C-3), 55.88 (C-22), 42.38 – 42.19 (C-24, C-25), 19.12 (C-21), 17.07 (C-19), 12.07 (C-18). ε$_{(262nm, DMSO)}$ = 3691 M^{-1}cm^{-1}. *Anal*. C 47.08%, N 10.50%, H 6.80%, calcd. for C$_{25}$H$_{42}$AuCl N$_4$O· CH$_3$CN: C 47.13%, N 10.18%, H 6.59%.

[Dinitrate-di(22-hydrazine-imidazoline-2-yl-chol-5-en-3β-ol) copper (II)] (**2**)

To a blue solution of copper(II) nitrate trihydrate (92.2 mg; 0.37 mmol) in methanol, was added **AH3** (103.6 mg; 0.25 mmol), the solution became light green. Then, the solution was placed under reflux at constant stirring for 2 hours. The solvent was filtrated and the green solid was washed with acetonitrile and diethyl ether. (139 mg. 55%). Amorphous power: mp 200-202 °C. IR (KBr) n$_{max}$ 3353, 2926, 1657, 1384, 1049 cm^{-1}. ^{1}H-NMR (DMSO-d$_6$, 500 MHz) δ 5.24 (1H, t, H-6), 4.57 (1H, s, NH), 3.63 (4H, s, H-23 and H-24), 0.89 (3H, s, H-21), 0.92 (3H, s, H-19), 0.66 (3H, s, H-18). ε$_{(262nm, DMSO)}$ = 4236 M^{-1}cm^{-1}. *Anal*. C 46.90%, N 13.13%, H 7.56%, calcd. for C$_{25}$H$_{46}$CuN$_6$O$_9$: C 47.05%, N 13.17%, H 7.26%.

Lipophylicity determination

The logarithm of the partition coefficient between *n*-octanol and water (Log *P*) is a universally accepted physicochemical model of these important biological effects, and is a very widely used parameter in medicinal chemistry [57]. The partition coefficient of the complex between n-octanol (*o*) and water (*w*) was studied by the shake-flask method. Drugs were dissolved at a concentration of 1 mM in the aqueous phase (3 mL). An equal volume of saturated *n*-octanol was added and the solutions were mixed in the water-bath for 30 min. The organic and aqueous phases were separated and the concentration of drug in each phase was measured by UV-visible. The logarithm of the ratio of compound concentration in the organic and aqueous phases was calculated to determine Log *P* values [58].

DNA interactions

All the measurements with calf thymus (ct) DNA were carried out in buffer Tris–HCl 5 mM (pH 7.2), 50 mM NaCl. The UV absorbance ratio λ$_{260}$/λ$_{280}$ was 1.8–1.9 indicating that the DNA was essentially free of protein [59]. The ct-DNA concentration per nucleotide was determined by absorption spectrophotometric analysis using the molar absorption coefficient 6600 mol^{-1}dm^{3}cm^{-1} at 260 nm [60].

The spectroscopic titrations were carried out by adding increasing amounts of ctDNA to a solution of the compound at a fixed concentration in a quartz cell, and recording the UV–Vis spectra after each addition. The absorption by DNA was subtracted by adding the same amounts of ct-DNA to the blank. The intrinsic binding constant K$_b$ was determined from the plot of [DNA]/(e$_a$ - e$_f$) vs [DNA], where [DNA] is the concentration of DNA in base pairs, and the apparent absorption

coefficients, ε_a, ε_f, ε_b correspond to A_{obs}/[compound], the extinction coefficient for the free compound and the extinction coefficient of the compounds in the totally bound form, respectively. The data were fitted to Eq. 1, with a slope equal to $1/(\varepsilon_b - \varepsilon_f)$ and the intercept equal to $1/[Kb(\varepsilon_b - \varepsilon_f)]$ and Kb was obtained from the ratio of the slope to the intercept [61].

$$[DNA] / (\varepsilon_a - \varepsilon_f) = [DNA] / (\varepsilon_b - \varepsilon_f) + 1 / [K_b (\varepsilon_b - \varepsilon_f)] \quad \text{(Eq. 1)}$$

The interaction of these compounds (**AH3**, **1** and **2**) with ct-DNA was also measured in thermal denaturation experiments. Melting curves were recorded in media containing 50 mM NaClO$_4$ and 5 mMTris/HCl buffer (pH = 7.29). The absorbance of the ct-DNA solution ($\sim 60 \ \mu M$) with Ri = 0.1 (relation [Compound]/[DNA]) was monitored at 260 nm before and after incubation with the drug ($\sim 7 \ \mu M$ in Tris/HCl buffer) for 1 h at room temperature. The temperature was increased by 1 ºC/min between 65 and 85 ºC and by 3ºC/min between 40 and 65 ºC and between 85 and 94 ºC [62].

Viscosity measurements were carried out using an Ostwald viscometer immersed in a water bath maintained at 25 °C. The DNA concentration was kept constant in all samples, while the compound concentration was increased from 0 to 67 μM. The flow time was measured at least 6 times with a digital stopwatch and the mean value was calculated. Data are presented as $(\eta/\eta^0)^{1/3}$ versus the ratio [compound]/[DNA], where η and η^0 are the specific viscosity of DNA in the presence and absence of the compound, respectively. The values of η and η^0 were calculated by use of the expression $(t - t^b)/t^b$, where t is the observed flow time and t^b is the flow time of buffer alone. The relative viscosity of the DNA was calculated from η/η_0 [63].

TrxR interaction

TrxR inhibition experiments were carried out using a TrxR rat liver kit and bovine serum albumin (BSA), both obtained from Sigma -Aldrich. The kit containing the EDTA phosphate buffer needed to carry out the experiment. Kinetic control was performed on a plate reader "TECAN Sunrise absorbance reader", using 96-well plates with flat bottom. A working buffer phosphate pH 7.0, with 20 mM EDTA, 20 μg/mL BSA and 0.5 μg/mL of enzyme TrxR rat liver was prepared. This buffer was distributed into the wells of the plate, and then incubated for 10 minutes at room temperature with different concentrations of compound dissolved in DMSO. In the case of the control sample, was added the same volume of DMSO to the working buffer. After this time, the reaction was initiated with the addition of 5,5´-dithiobis (2- nitrobenzoic acid) (DTNB , included in the kit), which when is reduced by the enzyme system provides a direct measurement of the TrxR activity [64]. The kinetics was studied for about 16 minutes, making measurements every 16 seconds. The IC$_{50}$ were calculated as the concentration of compound decreasing the enzymatic activity of the untreated control by 50%.

Antifungal activity tests

Yeasts of reference isolates *Sporothrix schenckii* CBS 132984 and *Sporothrix brasiliensis* CBS 133021 were obtained from filamentous form (saprophytic form) cultivated in potato agar dextrose agar (PDA) and then cultivated in brain heart infusion broth supplemented with 2% glucose, at 36°C, with orbital agitation (150 rpm) for 7 days. Antifungal activity of compounds were determined according to the minimum inhibitory concentrations (MIC), and compared to the gold standard drug itraconazole (Sigma Chemical Co.). MIC values were determined by broth microdilution test of the CLSI reference method M27-A3 adapted to *Sporothrix* spp. yeasts [13].

The compounds were kept as 20 mM stock solutions in DMSO at -20°C. Immediately before use, compounds were diluted in Roswell Park Memorial Institute (RPMI) 1640 medium supplemented with 2% glucose, into 96-well microliter, at final concentration ranging from 20 to 0.04 μM. Then, yeasts were added into microliter and a final yeast concentration ranging from 0.5-1x10^5 CFU (colonies form units)/mL were treated for 48 h, at 35°C, in a 5% CO$_2$ chamber. Minimum concentrations that inhibited pronouncedly fungal growth relative to untreated control were determined by visual inspection in an inverted light microscope, and confirmed by spectrophotometric readings at 490 nm, in a microliter plate reader (Molecular Devices SpectraMax Plus), corresponding to inhibitions as from 80%. These percentage of inhibition was calculated according following equation: $100 – (A \times 100/C)$, where A is the absorbance value of wells containing compound and C is absorbance of control wells. Results are representative of two independent experiments made in duplicate.

References

1. Pagán-Mercado, G.; Rivera-Ruiz, M. E.; Segarra-Román, F.; Rodríguez-Medina, J. R. *P. R. Health Sci. J.* **2009**, *28*, 220-226.
2. Urbina, J.; Vivas, J.; Visbal, G.; Contreras, L. M. *Mol. Biochem. Parasitol.* **1995**, *73*, 199-210.
3. Urbina, J. A.; Vivas, J.; Lazardi, K.; Molina, J.; Payares, G.; Piras, M. M.; Piras, R. *Chemotherapy.* **1996**, *42*, 294-307.

4. Haughan, P. A.; Change, M. L.; Goad, L. J. *Biochem. J.* **1995**, *308*, 31-38.

5. Rodrigues, J. C. F.; Bernardes, C. F.; Visbal, G.; Urbina, J. A.; Vercesi, A. E.; de Souza, W. *Protist.* **2007**, *158*, 447-456.

6. Visbal, G.; Marchan. E.; Maldonado, A.; Simoni, Z.; Navarro, M. *J. Inorg. Biochem.* **2008**, *102*, 547-554.

7. Urbina, J. A.; Visbal, G.; Contreras, L. M.; McLaughlin, G.; Do-Campo, R. *Antimicrob. Agents. Chemother.***1997**, *41*, 1428-1432.

8. Visbal, G.; Alvarez, A.; Moreno, B.; San-Blas, G. *Antimicrob. Agents. Chemother.***200 3,** *47*, 2966-2970.

9. Visbal, G.; San-Blas, G.; Maldonado, A.; Álvarez-Aular, A.; Capparelli, M. V.; Murgich, J. *Steroids.* **2011,***76*, 1069-1081.

10. Ishida, K.; Rodrigues, J. C. F.; Ribeiro, M. D.; Vila, T. V.; de Souza, W.; Urbina, J. A.; Nakamura, C. V.; Rozental, S.*B. M. C. Microbiol.* **2009**, *9*, 74.

11. Vivas, J.; Alvarado, P.; Visbal, G.; Alvarez-Aular, A.; Ruiz, E.; Ledezma, E. *Invest. Clin.* **2011**, *52*, 312-322.

12. Visbal, G.; San-Blas, G.; Murgich, J.; Franco, H. *Curr. Drug Targets: Infect Disorders.* **2005**, *5*, 211-226.

13. Borba-Santos, L.; Visbal, G.; Gagini, T.; Rodrigues, A M.; de Camargo, Z.; Lopes-Bezerra, L.; Ishida, K; de Souza, W.; Rozental, S. *Front. Microbiol.* (Online). **2016**, *7*:311, 1-13.

14. Sánchez-Delgado R.; Navarro M.; LazardiK.; UrbinaJ.; Atencio, R.; Noels, A. N. *Inorg. Chim. Acta.* **1998**, *275*, 528-540.

15. Sanchez-Delgado, R. A.; Anzellotti, A. *Mini rev. Med. Chem.* **2004**, *4*, 23-30.

16. Navarro, M.; Cisneros-Fajardo, E. J.; Lehmann, T.; Sánchez-Delgado, R.; Atencio, R.; Silva, P.; Lira, R.; Urbina, J. *Inorg.Chem.* **2001**, *40*, 6879-6884.

17. Navarro, M.; Lehmann, T.; Cisneros-Fajardo, E. J.; Fuentes, A.; Sánchez-Delgado, R.; Silva, P.; Urbina, J. *Polyhedrom.* **2000**, *19*, 2319-2325.

18. Iniguez, E.; Sánchez, A.; Vasquez, M. A.; Martínez, A.; Olivas, J.; Sattler, A.; Sánchez-Delgado, R. A.; Maldonado, R. A. *J. Biol. Inorg. Chem.* **2013**,*18*, 779-790.

19. Martínez, A.; Carreon, T.; Iniguez, E.; Anzellotti, A.; Sánchez, A.; Tyan, M.; Sattler, A.; Herrera, L.; Maldonado, R. A.; Sánchez-Delgado, R. A. *J. Med. Chem.* **2012**, *55*, 3867-3877.

20. Visbal, G.; Marchan, E.; Maldonado, A.; Simoni, Z.; Navarro, M. J. *Inorg. Biochem.*2008, *102*, 547-554

21. Navarro, M.; Marchán, E.; Maldonado, A.; Simoni, Z.; Velásquez, M.; Herrera, L.; Visbal, G. *Trans. Met. Chem.* **2015**, *40*, 707-713.

22. Long, E. C.; Barton, J. K. *Acc. Chem. Res.* **1990**, *23*, 271-273.

23. Pages, B. J.; Ang, D. L.; Wright, E. P.; Aldrich-Wright, J. R. *Dalton Trans.* **2015,** *44*, 3505-3526.

24. García-Ramos J. C.; Galindo-Murillo, R.; Cortés-Guzmán, F.; Ruiz-Azuara, L. *J. Mex. Chem. Soc.* **2013**, *57*, 245-259.

25. Navarro, M.; Castro, W.; González, S.; Abad, M. J.; Taylor, P. *J. Mex. Chem. Soc.* **2013**, *57*, 220-229.

26. Berners-Price, S. J.; Filipovska, A. *Metallomics,* **2011**, *3*, 863-873.

27. Nobili, S.; Mini, E.; Landini, I.; Gabbiani, C.; Casini, A.; Messori, L. *Med. Res. Rev.*, **2010**, *30*, 550-580.

28. Lessa, J. A.; Guerra, J. C.; de Miranda, L. F.; Romeiro, C. F. D.; Da Silva, J. G.; Mendes, I. C.; Speziali, N. L.; Souza-Fagundes, E. M.; Beraldo, H. *J. Inorg. Biochem.* **2011**, *105*, 1729-1739.

29. Liu, W.; Bensdorf, K.; Proetto, M.; Abram, U.; Hagenbach, A.; Gust, R. *J. Med. Chem.* **2011**, *54*, 8605-8615.

30. Chakrabarti, A.; Bonifaz, A.; Gutierrez-Galhardo, M. C.; Mochizuki, T.; Li, S.*Med. Mycol.* **2015**, *53*, 3-14.

31. Medici, N. P.; Del Poeta, M. *Mem Inst Oswaldo Cruz, Rio de Janeiro.* **2015**, *110*, 966-973.

32. Kauffman, C. A.; Bustamante, B.; Chapman, S. W.; Pappas, P. G. *Clin. Infect. Dis.* **2007**, *45*, 1255-1265.

33. Rodrigues, A. M.; de Hoog, G. S., de Cássia Pires, D.; Brilhante, R.S.; Gadelha, M. F.; Colombo, A. L.; de Camargo, Z. P. *BMC. Infect. Dis.* **2014**, *14*, 219.

34. Borba-Santos, L. P.; Rodrigues, A. M.; Gagini, T. B.; Fernandes, G. F.; Castro, R.; de Camargo, Z. P.; Nucci, M.; Lopes-Bezerra, L. M.; Ishida, K.; Rozental, S. *Med. Mycol.* **2015**, *53*, 178-188.

35. K. Nakamoto, Coordination Compounds. In Infrared and Raman Spectra of Inorganic and Coordination Compounds, 4th Ed.; John Wiley and Sons, Inc.: New York, (1986).

36. Wilkinson, G. *Comprehensive Coordination Chemistry.* Eds. Pergamon, **1987**.

37. Pages, B. J.; Ang, D. L.; Wright, E. P.; Aldrich-Wright, J. R. *Dalton Trans.* **2015**, 44**,** 3505-3526.

38. García-Ramos, J. C.; Galindo-Murillo, R.; Cortés-Guzmán, F.; Ruiz-Azuara, L. *J. Mex. Chem. Soc.* **2013**, 57(3), 245-259.

39. Topală, T.; Bodoki, A.; L Oprean, L.; Radu O. *Farmacia*, **2014**, Vol. 62, 6, 1049-1061.

40. Barton, J. K.; Danishefsky, A.; Goldberg, J. *J. Am. Chem. Soc.* **1987**, *106*, 2172.

41. Navarro M.; Corona, O.; Colmenares, I.; Marchan, E.; *Lett. Drug Des. Discov.* **2006**, 3:*7*, 454-458.

42. Ussery, D. W. *DNA Denaturation.* Academic Press, New York, **2001**.

43. Satyanarayana, S.; Dabrowiak, J. C.; Chaires, J. B. *Biochemistry.* **1992**, *31*, 9319-9324.

44. Navarro, M.; Betancourt, A.; Hernández, C.; Marchán, E. *J. Braz. Chem. Soc.* **2008**, *19*, 1355.

45. Cohen, G.; Eisemberg, H. *Biopolymers.* **1969**, *8*, 45-55.

46. Holmgren, A. Annu. Rev. Biochem. **1985**, *54*, 237-271.

47. Barry, N. P. E.; Sadler, P. *J. Chem. Commun.* **2013**, *49*, 5106-5131.

48. Liu, W.; Bensdorf, K.; Proetto, M.; Abram, U.; Hagenbach, A.; Gust, R. *J. Med. Chem.* **2011**, *54*, 8605-8615.

49. McKeage, M.; Berners-Price, S.; Galettis, P.; Bowen, R.; Brouwer, W.; Ding, L.; Zhuang, L.; Baguley, B. *Cancer Chemother. Pharmacol.* **2000**, *46*, 343-350.

50. Sarkarand, A.; Kellogg, G. E. *Curr. Top. Med. Chem.* **2010**, *10*(1): 67-83.

51. Leo, A.; Hansch, C.; Elkins, D. *Chem. Rev.* **1971**, *71*, 525-616.

52. Martínez, A.; Rajapakse, C. S. K.; Naoulou, B.; Kopkalli, Y.; Davenport, L.; Sánchez-Delgado, R. A. *J. Biol. Inorg. Chem.* **2008**, *13*, 703-712.

53. Martínez, A.; Rajapakse, C. S. K.; Jalloh, D.; Dautriche, C.; Sánchez-Delgado, R. A. *J. Biol. Inorg. Chem.* **2009**, *14*, 863-871.

54. Rodrigues, A. M.; de Melo Teixeira, M.; de Hoog, G.S.; Schubach, T. M. P.; Pereira, S. A.; Fernandes, G. F.; Lopes Bezerra, L. M.; Sueli Felipe, M.; de Camargo, Z. P. PLoS Negl. Trop. Dis. **2013**, *7*(6): e2281.

55. Zhang, Y.; Hagen, F.; Stielow, B.; Rodrigues, A. M.; Samerpitak, K.; Zhou, X.; Feng, P.; Yang, L.; Chen, M.; Deng, S.; Li, S.; Liao, W.; Li, R.; Li, F.; Meis, J. F.; Guarro, J.; Teixeira, M.; Al-Zahrani, H. S.; de Camargo, Z. P.; Zhang, L.; de Hoog, G. S. Persoonia. **2015**, *35*, 1-20.

56. Reis, É. G.; Schubach, T. M.; Pereira, S. A.; Silva, J. N.; Carvalho, B. W.; Quintana, M. S.; Gremião, I. D. *Med Mycol.* **2016**, *54*, 684-690.

57. Tetko, I. V.; Jaroszewicz, I.; Platts, J. A.; Kuduk-Jaworska, J. *J. Inorg.Biochem.* **2008**, 102, 1424-1437.

58. Hansch, C.; Bjorkroth, J. P.; Leo, A. *J. Pharm. Sci.* **1987**, *76*, 663-687.

59. Hay, P. J.; Wadt, W. R. *J. Chem. Phys.* **1985**, *82*, 299.

60. Marmur, J. *J. Mol. Biol.* **1961**, *3*, 208-218.

61. Reichmann, M. E.; Rice, S. A.; Thomas, C. A.; Doty.; P. *J. Am. Chem. Soc.* **1954**, *76*, 3047-3053.

62. Martínez, A.; Rajapakse, C. S. K.; Naoulou, B.; Kopkalli, Y.; Davenport, L.; Sánchez-Delgado, R. A. *J. Biol. Inorg. Chem.* **2008**, *13*, 703-712.

63. Navarro, M.; Hernandez, C.; Colmenares, I.; Hernandez, P.; Fernandez, E.; Sierraalta, A.; Marchan, E. *J. Inorg. Biochem.* **2007**, *101*, 111-116.

64. Fang, J.; Lu, J.; Holmgren, A. *J. Biol. Chem.* **2005**, *280*, 25284-25290.